Available online at www.sciencedirect.com
ScienceDirect
Ceramics International 38S (2012) S577–S580
CERAMICS INTERNATIONAL
www.elsevier.com/locate/ceramint

Photoluminescence and photocurrent characteristics of $Sr_{1-x}Ba_xAl_2O_4$: Eu^{2+}, Ni^{2+} phosphors

J.H. Kim [a], H.D. Jang [a], S.K. Kim [b], H.B. Lee [c], E.S. Kim [a,*]

[a] Department of Materials Engineering, Kyonggi University, Suwon 443-760, Republic of Korea
[b] Korea Institute of Ceramic Engineering and Technology, Seoul 153-801, Republic of Korea
[c] Department of Ceramic Engineering, Myongji University, Yongin 449-729, Republic of Korea

Available online 27 May 2011

Abstract

Effects of crystal structure on the photoluminescence (PL) and photocurrent (PC) characteristics of $Sr_{1-x}Ba_xAl_2O_4$: Eu^{2+}, Ni^{2+} phosphors were investigated as a function of Ba^{2+} content ($0.1 \leq x \leq 0.5$) and/or type of doping ions. PL of the specimens was blue-shifted with Ba^{2+} content. With increasing of Ba^{2+} content, the PC of the specimens was increased up to $x = 0.3$ and then decreased. These results could be attributed to crystallinity and structural changes from monoclinic spinel ($0.1 \leq x \leq 0.3$) to hexagonal tridymite ($0.4 \leq x \leq 0.5$). With doping of Ni^{2+} ion, the response time of PC was remarkably shortened while the intensity of PL was slightly decreased to the incident light, which are due to the formation of trap energy level in the band gap generate from Ni^{2+} ion.

Keywords: A. Sol–gel processes; D. Spinels; E. Sensors; $Sr_{1-x}Ba_xAl_2O_4$: Eu, Ni

1. Introduction

Recently, much attention has been paid to the europium activated alkaline aluminate oxide as typical phosphor materials [1–3]. These phosphor materials are available to the various applications, because of the high luminescent intensity, long lasting time, suitable emitting color and chemical stability, and so on [4]. These properties could be explained by electron transition between ground state $4f^7$ and $4f^65d^1$ excite state of Eu^{2+}, which is strongly affected by mother phase of materials. It is also expected that the characteristics of photoluminescence and photocurrent are dependent on the intrinsic properties of mother phase. However, europium activated alkaline aluminate oxide phosphors have fatal problem for the sensor applications with afterglow phenomenon because the hole trap level does not exist in energy band gap.

As to the various application of phosphors for visible light sensor and displays such as LCD, PDP and FED, the wide range of emission spectrum and high efficiency at low voltage are essentially required, along with the good performance characteristics such as high ratio of photocurrent to dark current, photocurrent stability with applied voltage and fast response time to the incident light.

It has been reported that $SrAl_2O_4$ showed high quantum efficiency and good stability, and $BaAl_2O_4$ showed fast dropping time [5]. Also, the wide range of emission spectrum could be expected from the solid solutions of $SrAl_2O_4$–$BaAl_2O_4$.

Nickel ion is a well known transition metal ion, which has complicated optical spectra such as f–f transition and d–d transition. Many excitation spectrum peaks and longer oscillator strength than that of europium ion were reported for the addition of nickel ion on the europium activated alkaline aluminate oxides [6].

Comparing to the photoluminescence (PL) and photocurrent (PC) characteristics of $SrAl_2O_4$–$BaAl_2O_4$ solid solutions doped with Eu^{2+}, the doping effects of Ni^{+} on those of $SrAl_2O_4$–$BaAl_2O_4$ have been investigated to search the new materials applicable to visible light sensor and various displays operated at low voltage in this study. Dependence of PL and PC on the crystal structure and crystallinity of the specimens was also discussed with respect to the response time to the incident light.

* Corresponding author. Tel.: +82 31 249 9764; fax: +82 31 244 6300.
E-mail address: eskim@kyonggi.ac.kr (E.S. Kim).

0272-8842/$36.00
doi:10.1016/j.ceramint.2011.05.101

2. Experimental procedures

$Sr_{1-x}Ba_xAl_2O_4$: Eu^{2+}, Ni^{2+} phosphor materials prepared by sol–gel process as a function of Ba^{2+} content with co-doped and/or type of doping ion. The raw materials $Al(NO_3)_3{\cdot}9H_2O$, $Sr(NO_3)_2$, and $Ba(NO_3)_2$ were dissolved in distilled water for 1 h. $Eu(NO_3)_3{\cdot}6H_2O$ and/or $Ni(CH_3COOH)_2$ were also dissolved in distilled water, respectively. The precursor solutions were uniformly mixed for the desired compositions with 0.01 mol of Eu^{2+} and/or Ni^{2+} and then vigorous stirring for 3 h. The precursor solution was poured into a crucible with a lid and introduced into oven at 110 °C for 12 h. The xerogel was calcined at 1200 °C for 10 h under a reducing atmosphere of 97% Ar with 3% H_2. These calcined powders were milled with ZrO_2 balls for 24 h in distilled water and then dried. Dried powders were pressed into 15 mm diameter disk at 1000 kg/cm^2 isostatically. Theses pellets were sintered at 1350 °C for 5 h under a reducing atmosphere of 97% Ar with 3% H_2. And then, sintered specimens were coated with Pt electrode, comb-like shape with the spacing of 0.3 mm.

Powder X-ray diffraction (XRD) analysis (D/Max-3C, Rigaku, Japan) was used to identify the phase of the specimens. Full width at half-maximum (FWHM) values of (2 2 0) peak were determined from XRD patterns. The luminescence properties of the specimens were measured by a photoluminescence (R6452, Advantest, Japan). The emission spectra of the specimens were obtained the excited light intensity as function of wavelength by Xe lamp. The photocurrent of the specimens was measured in a specially designed measuring box. Because $Sr_{1-x}Ba_xAl_2O_4$ co-doped with Eu^{2+} and/or Ni^{2+} specimens were very sensitive to visual light, the measuring box was shielded from the external visual light. 20 W-fluorescent lamps (Sankyo-denki, peak wavelength 368 nm, Japan) and D65 daylight fluorescent lamps (Gretagmacbeth, Canada) were used as a UV source and a visible light source, respectively. The UV and visual light intensity were controlled by adjusting the distance between light source and the sample according to the indication of UV radiometer (VLX-3W, Vilber Lourmat, France) and visible light meter (LX-1102, Lutron, Taiwan) placed beside the sample. The photocurrent was measured by a high resistance meter (R8340A, Advantest, Japan) with applied voltage from 0 to 40 (R6144, Advantest, Japan).

3. Results and discussion

The specimens of $Sr_{1-x}Ba_xAl_2O_4$ doped with Eu^{2+} and/or Ni^{2+} were prepared by sol–gel process. The specimens were sintered in H_2 reducing atmosphere at 1350 °C for 5 h. Fig. 1 shows the X-ray diffraction (XRD) pattern of $Sr_{1-x}Ba_xAl_2O_4$ doped with Ni^{2+} specimens. A single phase of spinel with monoclinic structure was observed at $x = 0.1$. With increasing of Ba^{2+} content, the crystal structure of the specimens was changed from monoclinic spinel to hexagonal tridymite for the specimens with $x > 0.3$.

As confirmed in the insert of Fig. 1, the X-ray diffraction peaks were shifted to lower 2θ ($2\theta = 28.44$–28.12°) with the

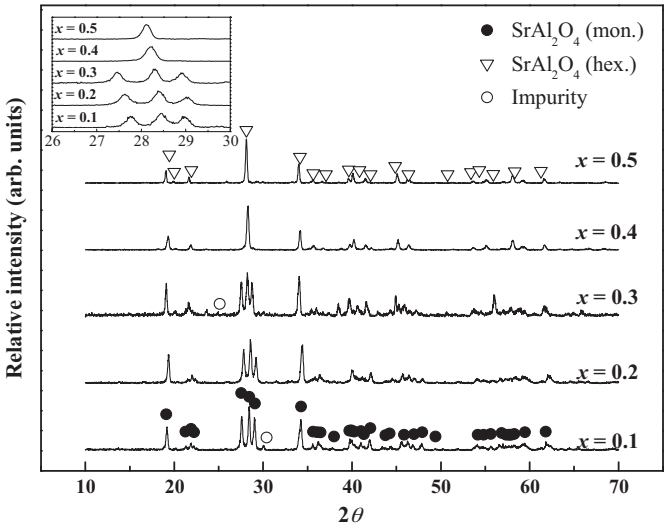

Fig. 1. XRD patterns of $Sr_{1-x}Ba_xAl_2O_4$ doped with Ni^{2+} specimens sintered at 1350 °C for 5 h.

increase of Ba^{2+} content, due to the larger ionic size of Ba^{2+} (1.50 Å) than those of Sr^{2+} (1.27 Å) and/or Eu^{2+} (1.30 Å) [7]. According to Wu et al. [8], the unit-cell volume of $Sr_{1-x}Ba_xAl_2O_4$ specimens was increased up to $x = 0.3$, and then drastically decreased for the further substitution of Ba^{2+} for Sr^{2+}. There is a small peak at $2\theta = 25.1^\circ, 31.2^\circ$ indicating the existence of $SrAl_4O_7$ or $SrCO_3$ as intermediate phase [9,10]. It has been reported that these peaks can be disappeared with increasing the sintering temperature up to 1400 °C [9]. XRD patterns of $Sr_{1-x}Ba_xAl_2O_4$: Eu^{2+} and $Sr_{1-x}Ba_xAl_2O_4$: Eu^{2+}, Ni^{2+} specimens showed a similar tendency of Fig. 1.

As shown in Fig. 2, the emission spectra of the specimens were blue-shifted ($\Delta\lambda_p \approx 10$ nm) with increasing of Ba^{2+} content due to crystal field effect [11]. The energy level was

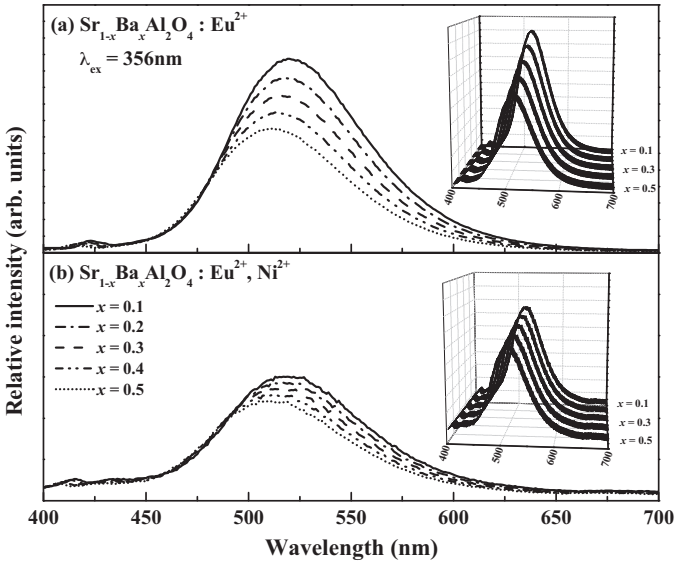

Fig. 2. Reflective emission spectra of (a) $Sr_{1-x}Ba_xAl_2O_4$: Eu^{2+} phosphor, (b) $Sr_{1-x}Ba_xAl_2O_4$: Eu^{2+}, Ni^{2+} phosphor.

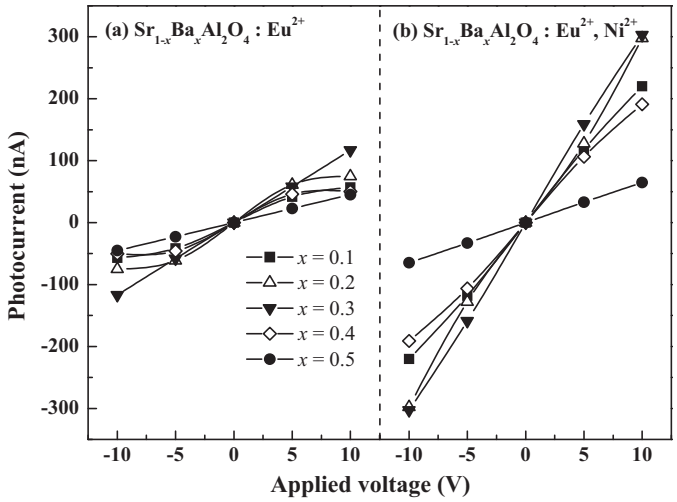

Fig. 3. Photocurrent of (a) $Sr_{1-x}Ba_xAl_2O_4$: Eu^{2+}, (b) $Sr_{1-x}Ba_xAl_2O_4$: Eu^{2+}, Ni^{2+} sintered specimens with applied voltage at 500 Lux.

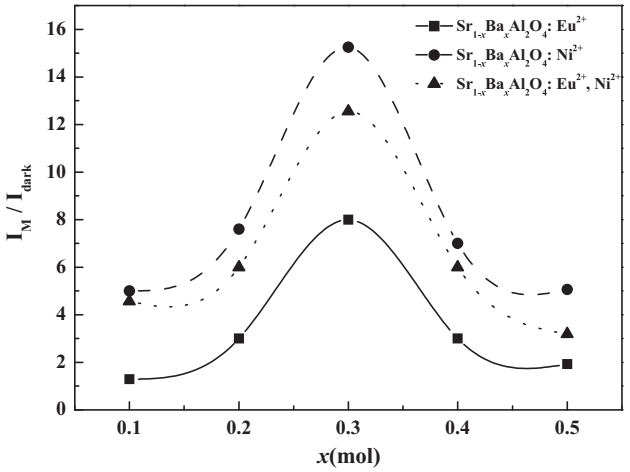

Fig. 4. Ratio of photocurrent (I_M) to dark current (I_{dark}) for $Sr_{1-x}Ba_xAl_2O_4$ sintered specimens at 10 V with 500 Lux.

splitted from $4f^7$ to $5d^1$ with substitution of Ba^{2+} for Sr^{2+} of $Sr_{1-x}Ba_xAl_2O_4$. It is well known that 5d electrons are very sensitive to the lattice environment [11]. Also, the characteristics of photoluminescence (PL) were strongly depended on the intrinsic properties of mother phase.

The intensity of the emission spectra was decreased with the substitution of Ba^{2+} for Sr^{2+} of $Sr_{1-x}Ba_xAl_2O_4$. And, the intensity of $Sr_{1-x}Ba_xAl_2O_4$ doped with Eu^{2+} specimens was higher than that of the specimens co-doped with Eu^{2+} and Ni^{2+} due to the formation of strong trap energy levels by Ni^{2+} ion in the energy band gap, which level interrupted the electron–hole recombination.

The characteristics of photocurrent (PC) of $Sr_{1-x}Ba_xAl_2O_4$: Eu^{2+} and $Sr_{1-x}Ba_xAl_2O_4$: Eu^{2+}, Ni^{2+} at illuminance of 500 Lux are shown in Fig. 3. The photocurrent of the specimens showed the linearity with applied voltage from −10 V to 10 V. For the entire range of compositions, the PC of the specimens were increased up to $x = 0.3$ and then decreased. It could be explained by crystallinity of the specimens which confirmed in Table 1. The crystallinity of the specimens was evaluated by full width at half-maximum (FWHM) of main peak (2 2 0) at $2\theta = 28.41^\circ$ of XRD patterns [12,13]. With increasing of crystallinity, the PC of the specimens was increased. Comparing to the PC of the specimens doped with Eu^{2+}, that of the specimens co-doped with Eu^{2+} and Ni^{2+} was remarkably improved. This result could possibly be attributed to the increase of hole transference. The hole transference should be increased because the electron–hole recombinations are inhibited by the strong trap energy levels with doping of Ni^{2+} ions.

Table 1
Full width at half-maximum (FWHM) of main peak (2 2 0) at $2\theta = 28.41^\circ$.

Composition	Dopant		
x (mol)	Eu^{2+}	Ni^{2+}	Eu^{2+}, Ni^{2+}
0.1	0.406	0.204	0.278
0.2	0.357	0.198	0.255
0.3	0.219	0.180	0.223
0.4	0.223	0.210	0.264
0.5	0.227	0.204	0.253

Fig. 4 shows the ratio (I_M/I_{dark}) of photocurrent (I_M) to dark current (I_{dark}) of the sintered specimens. The value of I_M/I_{dark} was increased with Ba^{2+} content up to $x = 0.3$, and then decreased for further substitution of Ba^{2+} for Sr^{2+}. The specimens with Ni^{2+} showed much higher value of I_M/I_{dark} than those of the specimens with Eu^{2+} and/or co-doped with Eu^{2+} and Ni^{2+}. These results could also be attributed to the formation of strong trap energy levels by Ni^{2+}.

Photocurrent responsivity of $Sr_{0.7}Ba_{0.3}Al_2O_4$: Eu^{2+}, Ni^{2+} specimens was measured for the light-on and light-off conditions at 10 V. As shown in Fig. 5, the photocurrent responsivity of the specimens at 10 V with 500 Lux was very fast and stable. When light-off, the PC of the specimens showed fast time response (<1 ms). Also, the photocurrent was very stable with 3 cycles of 500 Lux light-on and light-off during 1200s at 10 V.

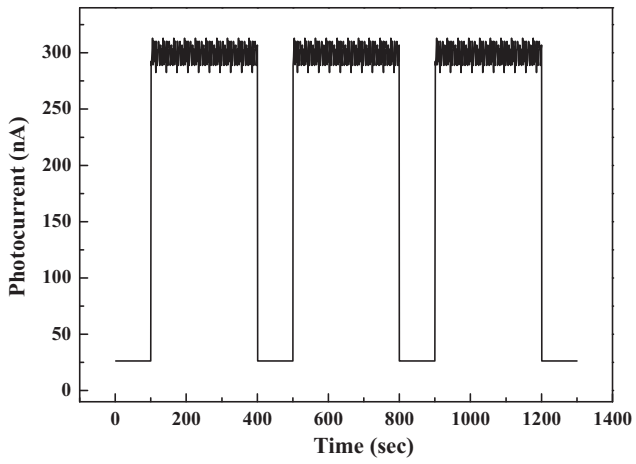

Fig. 5. Photocurrent responsivity of $Sr_{0.7}Ba_{0.3}Al_2O_4$: Eu^{2+}, Ni^{2+} at 10 V with 500 Lux.

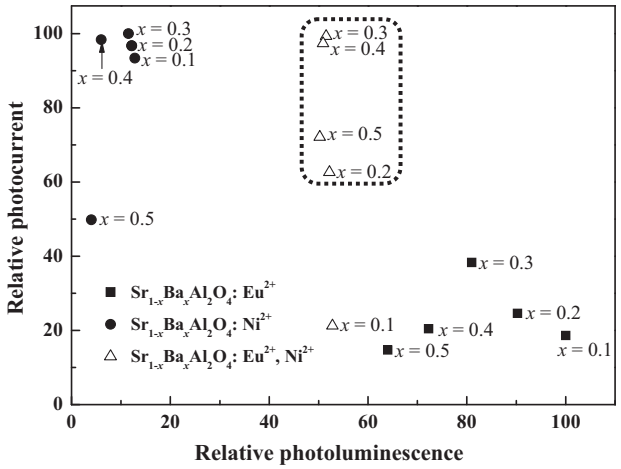

Fig. 6. The relationship between relative photocurrent and relative photoluminescence intensity of $Sr_{1-x}Ba_xAl_2O_4$ sintered specimens.

For the application of novelty technology, the photocurrent and photoluminescence characteristics of $Sr_{1-x}Ba_xAl_2O_4$: Eu^{2+}, Ni^{2+} have strong advantages. Especially, the specimens of $Sr_{0.7}Ba_{0.3}Al_2O_4$: Eu^{2+}, Ni^{2+} showed high photocurrent at low voltage. Fig. 6 shows the relationship between relative PC and relative PL intensity. In the range of dash line, the specimens of $Sr_{1-x}Ba_xAl_2O_4$: Eu^{2+}, Ni^{2+} specimens showed the characteristics of good PL and excellent PC, simultaneously, which suggested the possibility of novelty application.

4. Conclusions

The photoluminescence (PL) and photocurrent (PC) characteristics of $Sr_{1-x}Ba_xAl_2O_4$ phosphors were affected by Ba^{2+} content and doping of Ni^{2+} ion. With increasing of Ba^{2+} content, the crystal structure changes from monoclinic spinel ($0.1 \leq x \leq 0.3$) to hexagonal tridymite ($0.4 \leq x \leq 0.5$), and crystallinity was increase up to $x = 0.3$ and then decreased. The PL of the specimens was blue-shifted with the increase of Ba^{2+} content.

Ratio of photocurrent to dark current (I_M/I_{dark}) was increased up to $x = 0.3$, due to the intrinsic property of $BaAl_2O_4$. With doping of Ni^{2+} ion to $Sr_{1-x}Ba_xAl_2O_4$, the intensity of PL was decreased, while PC was increased. These results could be attributed to the formation of strong trap energy levels by Ni^{2+} ion in the energy band gap. Especially, the specimens of $Sr_{0.7}Ba_{0.3}Al_2O_4$: Eu^{2+}, Ni^{2+} showed the characteristics of good PL intensity and excellent PC, simultaneously.

References

[1] T.Y. Peng, L. Huajun, H.P. Yang, C.H. Yan, Synthesis of $SrAl_2O_4$: Eu, Dy phosphor nanometer powders by sol–gel processes and its optical properties, Materials Chemistry and Physics 85 (2004) 68–72.

[2] C.K. Chang, D.L. Mao, J.F. Shen, C.L. Feng, Preparation of long persistent $SrO{\cdot}2Al_2O_3$ ceramics and their luminescent properties, Journal of Alloys and Compounds 348 (2003) 224–230.

[3] J.Y. Zhang, Z.T. Zhang, T.M. Wang, W.C. Hao, Preparation and characterization of a new long afterglow indigo phosphor $Ca_{12}Al_{14}O_{33}$: Nd, Eu, Materials Letters 57 (2003) 4315–4318.

[4] Z.L. Fu, S.H. Zhou, Y.N. Yu, S.Y. Zhang, Combustion synthesis and luminescence properties of nanocrystalline monoclinic $SrAl_2O_4$: Eu^{2+}, Chemical Physics Letters 395 (2004) 285–289.

[5] S.K. Kim, M.J. Lee, J.H. Paik, B.H. Choi, Photoluminescence and photocurrent characteristics of Eu^{2+} activated MAl_2O_4 (M = Ba, Ca, Sr) phosphors, Journal of Electroceramics 17 (2006) 319–322.

[6] P. Yang, M.K. Lu, C.F. Song, S.W. Liu, D. Xu, D.R. Yuan, X.F. Cheng, Preparation and tunable photoluminescence characteristics of Ni^{2+}: $SrAl_2O_4$, Optical Materials 24 (2003) 575–580.

[7] R.D. Shannon, Revised effective ionic radii and systematic studies of interatomic distances in halides and chalcogenides, Acta Crystallographica A32 (1976) 751–767.

[8] Q. Wu, Z. Liu, H. Jiao, Luminescent properties of stabled hexagonal phase $Sr_{1-x}Ba_xAl_2O_4$: Eu^{2+} ($x = 0.37$–0.70), Physica B404 (2009) 2499–2502.

[9] Y.B. Xu, W.Y. Peng, S.J. Wang, X. Xiang, P.X. Lu, Synthesis of $SrAl_2O_4$ and $SrAl_{12}O_{19}$ via ethylenediaminetetraacetic acid precursor, Materials Chemistry and Physics 98 (2006) 51–54.

[10] T.Y. Peng, H.P. Yang, X.L. Pu, B. Hu, Z.C. Jiang, C.H. Yan, Combustion synthesis and photoluminescence of $SrAl_2O_4$: Eu, Dy phosphor nanoparticles, Materials Letters 58 (2004) 352–356.

[11] L.T. Chen, C.S. Hwang, I.L. Sun, I.G. Chen, Luminescence and chromaticity of alkaline earth aluminate $M_xSr_{1-x}Al_2O_4$:Eu^{2+} (M: Ca, Ba), Journal of Luminescence 118 (2006) 12–20.

[12] Z.L. Fu, S.H. Zhou, S.Y. Zhang, Study on optical properties of rare-earth ions in nanocrystalline monoclinic $SrAl_2O_4$:Ln (Ln = Ce^{3+}, Pr^{3+}, Tb^{3+}), Journal of Physical Chemistry B109 (2005) 14396–14400.

[13] C. Liu, Y.H. Wang, Y.H. Hu, R. Chen, F. Liao, Adjusting luminescence properties of $Sr_xCa_{1-x}Al_2O_4$: Eu^{2+}, Dy^{3+} phosphors by Sr/Ca ratio, Journal of Alloys and Compounds 470 (2009) 473–476.